Numerical Solution of the (1s1s) and (1s2s) Hydrogenic Pair Equations

Nicholas W. Winter
Battelle Memorial Institute, Columbus, Ohio 43201
and
Vincent McKoy
Arthur Amos Noyes Laboratory of Chemical Physics, California Institute of Technology, Pasadena, California 91109
(Received 7 May 1970)

The pair functions which determine the exact first-order wave function for the ground state of the three-electron atom have been found with the matrix finite-difference method. The second- and third-order energies for the $(1s1s)\,{}^1S$, $(1s2s)\,{}^3S$, and $(1s2s)\,{}^1S$ states of the two-electron atom are presented along with contour and perspective plots of the pair functions.

I. INTRODUCTION

It was previously shown that the functional coefficients of the partial-wave expansion for the first-order pair functions could be obtained with the matrix finite-difference (MFD) method.[1] Taking the full electron interaction as the perturbation, the method has been extended to the three pair equations that determine the first-order wave function for the lithium isoelectronic series.[2] The pair functions are independent of the nuclear charge and can be used to construct the first-order wave functions for other atoms when the remaining hydrogenic pair functions are determined.[3] The method is not variational and therefore can be applied without orthogonality constraints to the excited pair functions that are not the lowest of their symmetry. In addition, the calculation of the total second- and third-order energy involves none of the difficult integrals that occur for the complicated variational functions containing interelectronic coordinates.

The solution of the two-electron equations is described in Sec. II. The second- and third- order pair energies are compared to accurate variational results in Sec. III. Finally, the contour and perspective plots are presented for each of the pair functions.

II. SOLUTION OF FIRST-ORDER PAIR EQUATION

Since the pair functions are spherically symmetric, the partial-wave expansion for each is simply

$$U(r_1r_2\theta_{12})=\sum_l u_l(r_1r_2)P_l(\cos\theta_{12})\ . \tag{1}$$

By substituting this into the pair equation, multiplying both sides by $P_l(\cos\theta_{12})$, and integrating over the angular variables, the following partial differential equation for $u_l(r_1r_2)$ is obtained:

$$\left\{-\frac{1}{2}\left[\frac{1}{r_1^2}\ \frac{\partial}{\partial r_1}\left(r_1^2\ \frac{\partial}{\partial r_1}\right)+\frac{1}{r_2^2}\ \frac{\partial}{\partial r_2}\left(r_2^2\frac{\partial}{\partial r_2}\right)\right]-\frac{1}{r_1}-\frac{1}{r_2}+\frac{l(l+1)}{2r_1^2}+\frac{l(l+1)}{2r_2^2}-\epsilon_i-\epsilon_j\right\}u_l(r_1r_2)$$
$$=\left(E_1(\text{pair})\delta_{l0}-\frac{r_<^l}{r_>^{l+1}}\right)R(r_1r_2)\ , \tag{2}$$

where $E_1=\frac{5}{8}$ for the $(1s1s)$ pair, $E_1=\frac{137}{729}$ for the $(1s2s)^3S$ pair, and $E_1=\frac{169}{729}$ for the $(1s2s)^1S$ pair. The function R is the radial part of the zero-order function for each state. The boundary conditions on $u_l(r_1r_2)$ require that it be finite for r_1 or $r_2=0$ and that it vanish for r_1 or $r_2=\infty$. The set of equations for the functional coefficients are not coupled and are solved independently for each partial wave using the MFD method.

The details of the numerical analysis have already been discussed[1,4,5]; however, two important modifications have been introduced which allow the diffuse excited states to be handled efficiently. First, the radial cutoff [the point at which $u_l(r_1r_2)$ is required to vanish] for these states must be taken farther out than for the $(1s1s)$ pair previously treated. Therefore, even with extrapolation, a very large number of points are needed to achieve comparable accuracy. To avoid this difficulty, the following coordinate transformation was introduced into the pair equation:

$$r_1=x_1^2\ ,\quad r_2=x_2^2\ . \tag{3}$$

The grid points in the transformed system are closely spaced near the nucleus and farther apart in the tail regions, as viewed in the untransformed system. This means that by using a large radial cutoff and relatively few points, the regions important to the accurate solution of (2) are not neglected.

The second modification in the MFD method was to improve the difference approximation of the derivatives. Instead of truncating the difference expansion at the second difference approximation, the fourth difference is included, giving the following improved approximation for the second derivative:

TABLE I. Extrapolation of the partial-wave contributions to E_2 for the $(1s1s)\,{}^1S$ pair.[a]

	S wave			P wave		
30	−0.126 799 67			30	−0.030 387 09	
		−0.125 933 07			−0.026 230 53	
45	−0.126 318 23		−0.125 256 67	45	−0.028 077 89	−0.026 493 39
		−0.125 425 77	−0.125 354 12		−0.026 427 67	−0.026 495 22
60	−0.125 927 78		−0.125 338 53	60	−0.027 355 92	−0.026 494 93
		−0.125 369 94			−0.026 470 72	
75	−0.125 726 96			75	−0.027 037 25	
	D wave			F wave		
30	−0.004 986 19			30	−0.001 606 36	
		−0.003 856 49			−0.001 063 41	
45	−0.004 358 58		−0.003 897 85	45	−0.001 304 72	−0.001 070 88
		−0.003 887 51	−0.003 904 19		−0.001 069 02	−0.001 075 72
60	−0.004 152 49		−0.003 903 18	60	−0.001 201 60	−0.001 074 95
		−0.003 897 54			−0.001 072 82	
75	−0.004 060 71			75	−0.001 155 24	
	G wave			I wave		
30	−0.000 715 73			30	−0.000 384 66	
		−0.000 404 80			−0.000 189 10	
45	−0.000 542 99		−0.000 401 41	45	−0.000 276 02	−0.000 182 05
		−0.000 402 26	−0.000 404 31		−0.000 183 81	−0.000 183 52
60	−0.000 481 42		−0.000 403 85	60	−0.000 235 68	−0.000 183 29
		−0.000 403 28			−0.000 183 48	
75	−0.000 453 29			75	−0.000 216 89	

[a]Results were obtained on a linear grid with a 12-a.u. cutoff using second differences only.

TABLE II. Extrapolation of the partial-wave contributions to E_2 for the $(1s2s)\,{}^3S$ pair.[a]

	S wave			P wave		
30	−0.026 634 38			25	−0.002 041 99	
		−0.041 345 52			−0.001 906 03	
60	−0.037 667 74		−0.044 774 54	50	−0.001 940 02	−0.001 910 20
		−0.044 393 54	−0.045 257 66		−0.001 909 74	−0.001 909 83
90	−0.041 404 30		−0.045 227 47	75	−0.001 923 20	−0.001 909 85
		−0.045 018 99			−0.001 909 82	
120	−0.042 985 73			100	−0.001 917 35	
	D wave			F wave		
25	−0.000 148 64			25	−0.000 023 76	
		−0.000 146 41			−0.000 024 18	
50	−0.000 146 96		−0.000 145 58	50	−0.000 024 07	−0.000 023 86
		−0.000 145 67	−0.000 145 58		−0.000 023 89	−0.000 023 85
75	−0.000 146 25		−0.000 145 58	75	−0.000 023 98	−0.000 023 85
		−0.000 145 61			−0.000 023 86	
100	−0.000 145 96			100	−0.000 023 92	
	G wave			I wave		
25	−0.000 005 60			25	−0.000 001 67	
		−0.000 006 02			−0.000 001 96	
50	−0.000 005 92		−0.000 005 89	50	−0.000 001 89	−0.000 001 88
		−0.000 005 90	−0.000 005 88		−0.000 001 89	−0.000 001 86
75	−0.000 005 91		−0.000 005 88	75	−0.000 001 89	−0.000 001 86
		−0.000 005 89			−0.000 001 86	
100	−0.000 005 89			100	−0.000 001 88	

[a]Results for the S wave were obtained on a linear grid with a 24-a.u. cutoff. Remaining waves were obtained with a 20-a.u. cutoff. Both calculations used second differences only.

TABLE III. Extrapolation of the partial-wave contributions to E_2 for the (1s2s) ^1S pair.[a]

		S wave			
30	−0.054 419 13				
		−0.100 338 59			
60	−0.088 858 73		−0.105 416 39		
		−0.104 851 29		−0.106 479 34	
90	−0.097 743 99		−0.106 412 91		
		−0.106 022 73			
120	−0.101 365 94				
			P wave		
25	−0.010 255 75				
		−0.006 229 71			
50	−0.007 236 23		−0.006 461 83		
		−0.006 436 04		−0.006 500 48	
75	−0.006 791 67		−0.006 498 06		
		−0.006 482 56			
100	−0.006 656 44				
			D wave		
25	−0.001 818 52				
		−0.000 895 50			
50	−0.001 126 26		−0.000 922 40		
		−0.000 919 42		−0.000 928 06	
75	−0.001 011 35		−0.000 927 70		
		−0.000 925 63			
100	−0.000 973 84				
			F wave		
25	−0.000 619 22				
		−0.000 257 69			
50	−0.000 348 08		−0.000 251 14		
		−0.000 251 87		−0.000 252 69	
75	−0.000 294 63		−0.000 252 59		
		−0.000 252 41			
100	−0.000 276 16				
			G wave		
25	−0.000 283 76				
		−0.000 104 62			
50	−0.000 149 41		−0.000 094 72		
		−0.000 095 82		−0.000 094 50	
75	−0.000 119 63		−0.000 094 51		
		−0.000 094 84			
100	−0.000 108 79				
			I wave		
25	−0.000 153 85				
		−0.000 052 21			
50	−0.000 077 61		−0.000 043 79		
		−0.000 044 73		−0.000 042 86	
75	−0.000 059 34		−0.000 042 92		
		−0.000 043 37			
100	−0.000 052 36				

[a]Results for the *S* wave were obtained on a linear grid with a 24-a.u. cutoff. Remaining waves were obtained with a 20-a.u. cutoff. Both calculations used second differences only.

$$u''(x_0) = (1/h^2)\left[-\tfrac{1}{12}u(x_0+2h) + \tfrac{4}{3}u(x_0+h) - \tfrac{15}{6}u(x_0) + \tfrac{4}{3}u(x_0-h) - \tfrac{1}{12}u(x_0-2h)\right] + O(h^4), \quad (4)$$

where h is the grid size. The only difficulty occurs at the boundary points, where (4) requires values of the function outside the defined grid. This was resolved with the following approximations: At the point $x = x_{max} - h$, where x_{max} is the radial cutoff, $u(x+2h)$ was set to zero; and at $x = h$, the value $u(x-2h)$ was set equal to $u(x)$. The latter assumption was arrived at by investigating the power-series form of $u(x)$ for small x and can be shown to introduce an error of the order of the difference truncation error, if the coordinate transformation (3) is used. An alternative would be to use the usual second-difference approximation at the boundaries and the fourth-difference approximation elsewhere. Actually, both approaches were used, depending on which method was used to solve the difference equations.

When substituted into (17), both the second-difference and the fourth-difference approximations lead to a set of simultaneous equations of the form

TABLE IV. Extrapolated results for the (1s1s) pair on the square-root grid.

N	20	25	30	35	40	Extrapolant
$E_2(0)$	−0.131 200 97	−0.128 659 71	−0.127 479 45	−0.126 835 08	−0.126 444 47	−0.125 327 22
$E_2(1)$	−0.031 534 28	−0.029 571 17	−0.028 571 86	−0.027 993 78	−0.027 628 63	−0.026 494 91
$E_2(2)$	−0.005 816 06	−0.005 072 96	−0.004 689 10	−0.004 467 20	−0.004 327 90	−0.003 905 32
$E_2(3)$	−0.002 076 65	−0.001 699 97	−0.001 497 40	−0.001 378 21	−0.001 302 91	−0.001 075 61
$E_2(4)$	−0.001 002 59	−0.000 788 35	−0.000 667 55	−0.000 594 41	−0.000 547 46	−0.000 402 68
$E_2(5)$	−0.000 569 40	−0.000 438 70	−0.000 361 70	−0.000 313 61	−0.000 282 08	−0.000 180 91
$E_2(6)$	−0.000 356 92	−0.000 272 84	−0.000 221 47	−0.000 188 44	−0.000 166 30	−0.000 091 72
$E_2(7)$	−0.000 239 10	−0.000 182 57	−0.000 147 04	−0.000 123 61	−0.000 107 57	−0.000 050 80
$E_2(8)$	−0.000 168 10	−0.000 128 62	−0.000 103 29	−0.000 086 23	−0.000 074 33	−0.000 030 23
$E_2(9)$	−0.000 122 65	−0.000 094 17	−0.000 075 62	−0.000 062 91	−0.000 053 90	−0.000 019 15
$\sum_I E_2$	−0.173 086 72	−0.166 909 07	−0.163 814 50	−0.162 043 39	−0.160 935 55	−0.157 578 56
E_3	0.010 519 00	0.007 869 48	0.006 609 95	0.005 914 83	0.005 491 80	0.004 286 06
E	−2.912 567 72	−2.909 039 59	−2.907 204 55	−2.906 128 56	−2.905 443 75	−2.903 292 49

TABLE V. Extrapolated results for the $(1s2s)\,^3S$ pair on the square-root grid.

N	20	25	30	35	40	Extrapolant
$E_2(0)$	−0.055 954 14	−0.051 297 46	−0.049 198 49	−0.048 055 44	−0.047 359 00	−0.045 318 08
$E_2(1)$	−0.001 911 19	−0.001 910 69	−0.001 910 38	−0.001 910 20	−0.001 910 11	−0.001 909 94
$E_2(2)$	−0.000 143 81	−0.000 144 92	−0.000 145 29	−0.000 145 44	−0.000 145 51	−0.000 145 59
$E_2(3)$	−0.000 022 71	−0.000 023 40	−0.000 023 64	−0.000 023 75	−0.000 023 80	−0.000 023 86
$E_2(4)$	−0.000 005 20	−0.000 005 58	−0.000 005 73	−0.000 005 80	−0.000 005 83	−0.000 005 87
$E_2(5)$	−0.000 001 48	−0.000 001 68	−0.000 001 77	−0.000 001 82	−0.000 001 84	−0.000 001 87
$E_2(6)$	−0.000 000 48	−0.000 000 59	−0.000 000 65	−0.000 000 68	−0.000 000 69	−0.000 000 71
$E_2(7)$	−0.000 000 17	−0.000 000 23	−0.000 000 26	−0.000 000 28	−0.000 000 29	−0.000 000 31
$E_2(8)$	−0.000 000 07	−0.000 000 10	−0.000 000 12	−0.000 000 13	−0.000 000 14	−0.000 000 15
$E_2(9)$	$-0.000\,000\,02_6$	$-0.000\,000\,04_3$	$-0.000\,000\,05_5$	$-0.000\,000\,06_3$	$-0.000\,000\,06_8$	−0.000 000 08
$\sum_l E_2$	−0.058 039 28	−0.053 384 68	−0.051 286 39	−0.050 143 59	−0.049 447 27	−0.047 406 47
E_3	−0.006 650 06	−0.004 581 20	−0.003 767 79	−0.003 353 43	−0.003 110 29	−0.002 438 36
E	−2.188 831 99	−2.182 108 55	−2.179 196 85	−2.177 639 68	−2.176 700 23	−2.173 987 49

$$\underline{D}\cdot\underline{u}=\underline{b}\,, \tag{5}$$

where $\underline{D}$ is a banded matrix. The second-difference approximation produces a symmetric matrix, as does the fourth-difference approximation with the modified boundary conditions. However, the mixed-difference method leads to an unsymmetric matrix. The difference equations were solved with Gaussian elimination for the $l=0$ partial wave and with the Gauss-Seidel method for $l>0$. It was found that for the higher partial-wave equations, the Gauss-Seidel method converged extremely fast, while for the S wave, the method diverged. Because the Gaussian elimination method is more efficient for symmetric matrices, the mixed-difference approximation was not used for the S wave, but was used for each of the higher waves.

III. CALCULATION OF SECOND- AND THIRD-ORDER ENERGIES FOR TWO-ELECTRON STATES

The partial-wave equations for each pair function were solved using both the usual second-difference approximation and the improved difference formula given by (19). The second-order energy for each pair was found from

$$E_2(\text{pair})=\sum_l \frac{1}{2l+1}\int u_l(r_1r_2)\left(\frac{r_<^l}{r_>^{l+1}}-E_1(\text{pair})\right)\times R(r_1r_2)r_1^2r_2^2\,dr_1\,dr_2\,. \tag{6}$$

The radial integral was calculated by the trapezoidal rule. The calculations were carried out at several grid sizes, and the results were extrapolated with Richardson's[6] method. Therefore, the difference and quadrature errors were eliminated in one step. Note that the perturbation energies are defined according to $E=\sum_n E_n Z^{-n}$.

The extrapolation tables for the partial-wave contributions to E_2 for the $(1s1s)$ pair are given in Table I. The results were found using the second-difference approximation and the untransformed (linear) grid with a 12-a.u. cutoff. The first column of each table lists the number of strips used in each direction. The second column gives the initial results, and the remaining columns contain the extrapolants. The latter were obtained using different sets of results from the first column. By displaying the results in this

TABLE VI. Extrapolated results for the $(1s2s)\,^1S$ pair on the square-root grid.

N	20	25	30	35	40	Extrapolant
$E_2(0)$	−0.139 424 67	−0.125 105 29	−0.118 632 54	−0.115 101 83	−0.112 948 19	−0.106 621 65
$E_2(1)$	−0.007 343 60	−0.007 008 53	−0.006 840 48	−0.006 744 12	−0.006 683 65	−0.006 497 85
$E_2(2)$	−0.001 256 44	−0.001 128 58	−0.001 062 79	−0.001 024 85	−0.001 001 08	−0.000 929 29
$E_2(3)$	−0.000 425 50	−0.000 360 86	−0.000 326 10	−0.000 305 63	−0.000 292 69	−0.000 253 55
$E_2(4)$	−0.000 197 94	−0.000 161 10	−0.000 140 39	−0.000 127 84	−0.000 119 77	−0.000 094 73
$E_2(5)$	−0.000 109 76	−0.000 087 06	−0.000 073 81	−0.000 065 56	−0.000 060 15	−0.000 042 67
$E_2(6)$	−0.000 067 84	−0.000 053 01	−0.000 044 11	−0.000 038 42	−0.000 034 62	−0.000 021 78
$E_2(7)$	−0.000 045 12	−0.000 034 98	−0.000 028 74	−0.000 024 68	−0.000 021 92	−0.000 012 19
$E_2(8)$	−0.000 031 63	−0.000 024 42	−0.000 019 92	−0.000 016 93	−0.000 014 87	−0.000 007 34
$E_2(9)$	−0.000 023 07	−0.000 017 79	−0.000 014 44	−0.000 012 19	−0.000 010 62	−0.000 004 69
$\sum_l E_2$	−0.148 925 58	−0.133 981 62	−0.127 183 31	−0.123 462 06	−0.121 187 56	−0.114 485 74
E_3	0.000 715 79	0.002 951 08	0.003 667 29	0.003 993 78	0.004 173 63	0.004 625 79
E	−2.184 560 96	−2.167 381 71	−2.159 867 19	−2.155 819 44	−2.153 365 09	−2.146 211 12

TABLE VII. Comparison of perturbation energies for the (1s1s) pair.

	Second differences[a]	Fourth differences[b]	BJ (Ref. 8.)	KS (Ref. 7)
$E_2(0)$	−0.125 339	−0.125 327	−0.125 334	−0.125 332
$E_2(1)$	−0.026 495	−0.026 495	−0.026 495	−0.026 446
$E_2(2)$	−0.003 904	−0.003 905	−0.003 906	−0.003 612
$E_2(3)$	−0.001 076	−0.001 076	−0.001 077	···
$E_2(4)$	−0.000 404	−0.000 403	−0.000 405	···
$E_2(5)$	−0.000 184	−0.000 181	−0.000 183	···
$E_2(6)$	−0.000 094	−0.000 092	−0.000 093	···
$E_2(7)$	−0.000 054	−0.000 051	−0.000 053	···
$E_2(8)$	−0.000 033	−0.000 030	−0.000 032	···
$E_2(9)$	−0.000 021	−0.000 019	−0.000 021	···
$E_2(10)$	−0.000 015	···	−0.000 014	···
$\sum_l E_2(l)$	−0.157 619	−0.157 579	−0.157 656	−0.157 666[c]
E_3	0.008 478	0.008 572	···	0.008 699

[a]Second-difference results were obtained on a linear grid with a 12-a.u. cutoff.

[b]Fourth difference results were obtained on a square-root grid with a 32-a.u. cutoff.

[c]The total E_2 was not obtained from a partial-wave expansion for this calculation.

TABLE IX. Comparison of perturbation energies for the (1s2s) ^1S pair.

	Second differences[a]	Fourth differences[b]	BJ (Ref. 8)	KS (Ref. 7)
$E_2(0)$	−0.106 479	−0.106 622	−0.106 335	
$E_2(1)$	−0.006 500	−0.006 498	−0.006 239	
$E_2(2)$	−0.000 928	−0.000 929	−0.000 816	
$E_2(3)$	−0.000 253	−0.000 254	−0.000 199	
$E_2(4)$	−0.000 095	−0.000 095	−0.000 066	
$E_2(5)$	−0.000 043	−0.000 043	−0.000 027	
$E_2(6)$	···	−0.000 022	···	
$E_2(7)$	···	−0.000 012	···	
$E_2(8)$	···	−0.000 007	···	
$E_2(9)$	···	−0.000 005	···	
$\sum E_2(l)$	−0.114 339	−0.114 486	−0.113 723	−0.114 476[c]
E_3	0.012 114	0.009 251	0.007 000	0.009 415

[a]Second-difference results were obtained on a linear grid with a 20-a.u. cutoff except for the S wave, which was calculated with a 24-a.u. cutoff.

[b]Fourth-difference results were obtained on a square-root grid with a 32-a.u. cutoff.

[c]Total E_2 was not obtained from a partial-wave expansion for this calculation.

manner, it is possible to determine whether the extrapolants are converging from above or below the true value. The partial-wave contributions from all but the S wave are converging from below and have converged to at least six decimal places. The results for the S wave appear to oscillate, but the subtable produced by the 45-, 60-, and 75-strip calculations is converging smoothly from below. The extrapolation tables for the ^3S and ^1S excited states are given in Tables II and III. These results illustrate the need for the modifications that were discussed in Sec. II. The 120-strip S-wave calculation required the solution of nearly 14 000 linear equations which took about 1 h on the IBM 360-75. The S-wave cutoff was taken at 24 a.u., which was still not far enough from the nucleus. Clearly, it was not practical to re-solve the equations with a larger cutoff. The functions for $l > 0$ were much less diffuse and could be obtained easily in only a few minutes. For the ^3S state, these waves were nearly converged without extrapolation. The S wave for both states converged from above.

TABLE VIII. Comparison of perturbation energies for the (1s2s) ^3S pair.

	Second differences[a]	Fourth differences[b]	BJ (Ref. 8)	KS (Ref. 7)
$E_2(0)$	−0.045 258	−0.045 318	−0.045 316	−0.045 318
$E_2(1)$	−0.001 909	−0.001 910	−0.001 898	−0.001 902
$E_2(2)$	−0.000 146	−0.000 146	−0.000 137	−0.000 135
$E_2(3)$	−0.000 024	−0.000 024	−0.000 020	···
$E_2(4)$	−0.000 006	−0.000 006	−0.000 004	···
$E_2(5)$	−0.000 002	−0.000 002	−0.000 001	···
$E_2(6)$	···	$-0.000\,000_7$	···	···
$E_2(7)$	···	$-0.000\,000_3$	···	···
$E_2(8)$	···	$-0.000\,000_2$	···	···
$E_2(9)$	···	$-0.000\,000_1$	···	···
$\sum_1 E_2(l)$	−0.047 345	−0.047 406	−0.047 377	−0.047 409[c]
E_3	−0.003 732	−0.004 876	−0.005 000	−0.004 872

[a]Second-difference results were obtained on a linear grid with a 20-a.u. cutoff except for the S wave, which was calculated with a 24-a.u. cutoff.

[b]Fourth-difference results were obtained on a square-root grid with a 32-a.u. cutoff.

[c]Total E_2 was not obtained from a partial-wave expansion for this calculation.

The three-pair equations were re-solved using the fourth-difference approximation and the transformed (square root) grid. The initial results and the final extrapolants for the first 10 partial-wave contributions to E_2 are given for the three states in Tables IV–VI. In addition, the third-order and total energies are also given for $Z = 2$. The radial cutoff was taken at 32 a.u. for all three calculations. The first important result that should be noted is that relatively few points were needed to obtain better accuracy than the linear-grid calculations. All of the numbers were found at one time with the same program, and the total time was about 1 h. This could have been reduced to about 20 min, if fewer grids were used. For example, the results from the 20-, 25-, and 30-strip calculations gave the following extrapolants for the (1s1s) pair:

$$E_2(0) = -0.125\,32 \text{ a.u.},$$

$$E_2(1) = -0.026\,48 \text{ a.u.},$$

$$E_2(2) = -0.003\,87 \text{ a.u.},$$

TABLE X. Values of the most positive and negative contours and the contour interval for the plots.

	$(1s1s)\,^1S$			$(1s2s)\,^3S$			$(1s2s)\,^1S$		
l	Interval	Positive	Negative	Interval	Positive	Negative	Interval	Positive	Negative
0	0.027 76	0.116 86	−0.299 53	0.018 19	0.136 41	−0.136 41	0.029 36	0.239 54	−0.200 93
1	0.009 36	•••	−0.140 46	0.003 16	0.023 73	−0.023 73	0.006 79	0.050 66	−0.051 17
2	0.003 59	•••	−0.053 83	0.000 90	0.006 73	−0.006 73	0.002 83	0.022 19	−0.020 29
3	0.001 94	•••	−0.029 17	0.000 37	0.002 77	−0.002 77	0.001 60	0.012 49	−0.011 55
4	0.001 25	•••	−0.018 69	0.000 19	0.001 39	−0.001 39	0.001 05	0.008 08	−0.007 65
5	0.000 88	•••	−0.013 23	0.000 11	0.000 80	−0.000 80	0.000 75	0.005 68	−0.005 51
ψ_0	0.071 87	1.078 08	•••	0.061 83	0.463 70	−0.463 70	0.059 65	0.462 63	−0.432 18
ψ_1	0.039 23	0.096 99	−0.491 43	0.020 42	0.153 18	−0.153 18	0.038 94	0.288 17	−0.295 93
ψ	0.047 16	0.707 33	•••	0.056 99	0.427 44	−0.427 44	0.047 99	0.264 58	−0.455 32

which agree well with the best results.

The third-order energy for each pair was calculated from

$$E_3(\text{pair}) = \sum_{l,l',k} \Omega^k(l0,l'0) \int u_l(r_1r_2)\,\frac{r_<^k}{r_>^{k+1}} \times u_{l'}(r_1r_2)\, r_1^2\, r_2^2\, dr_1\, dr_2 - E_1(\text{pair}) \sum_l \frac{1}{2l+1} \cdot \int u_l(r_1r_2) \times u_l(r_1r_2)\, r_1^2\, r_2^2\, dr_1\, dr_2 - 2E_2(\text{pair}) \int u_0(r_1r_2) \times R(r_1r_2) r_1^2\, r_2^2\, dr_1\, dr_2 \,, \tag{7}$$

where

$$\Omega^k(l0,l'0) = \int P_l(\cos\theta_{12})\, P_k(\cos\theta_{12}) \times P_{l'}(\cos\theta_{12})\, d(\cos\theta_{12}) \,.$$

The total energies were found for the helium atom and compare well to the following values given by Knight and Scherr[7]:

$$E(1s1s,\,^1S) = -2.903\,316\,92 \text{ a.u.} \,,$$

$$E(1s2s,\,^3S) = -2.173\,987\,77 \text{ a.u.} \,,$$

$$E(1s2s,\,^1S) = -2.146\,119\,80 \text{ a.u.}$$

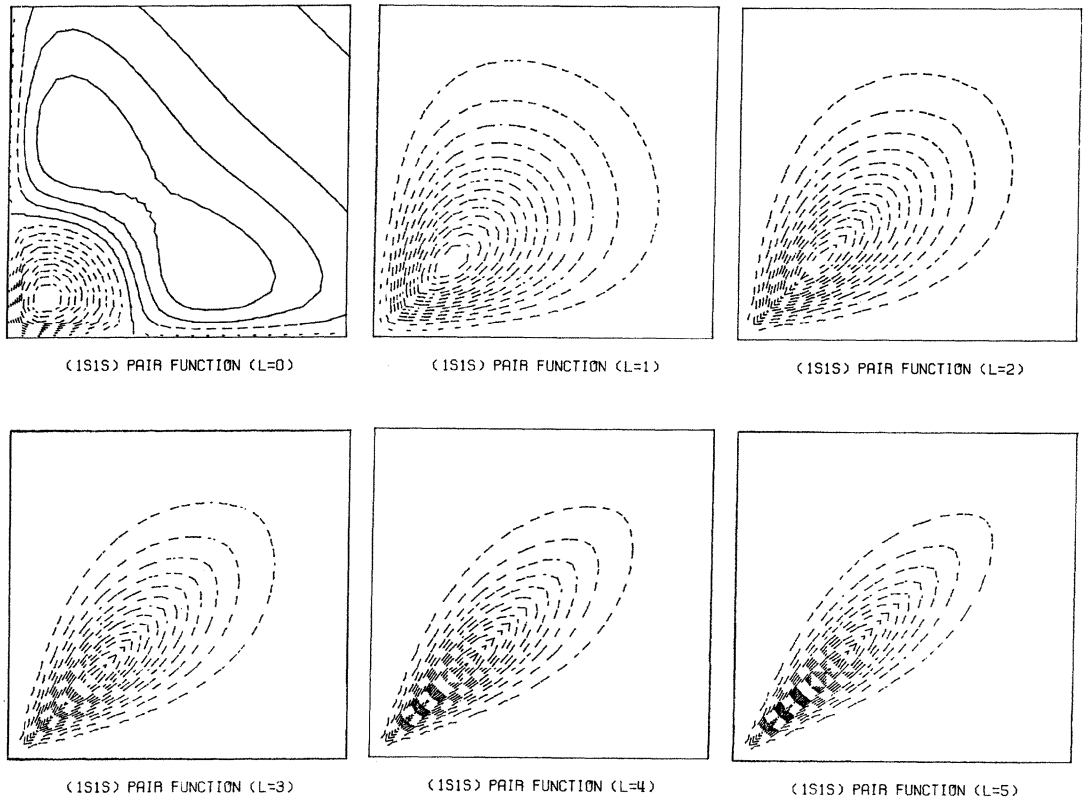

FIG. 1. Contour plots of functional coefficients for the $(1s1s)$ pair.

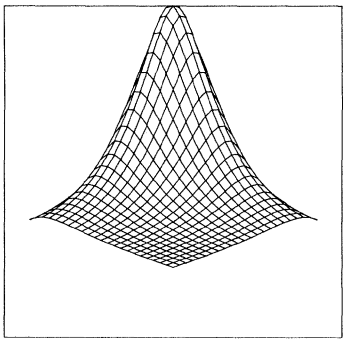

(1S1S) HYDROGENIC ZERO-ORDER FUNCTION

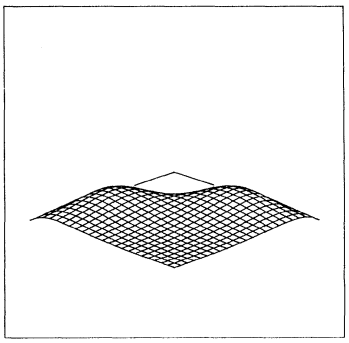

(1S1S) PAIR FUNCTION (L=0)

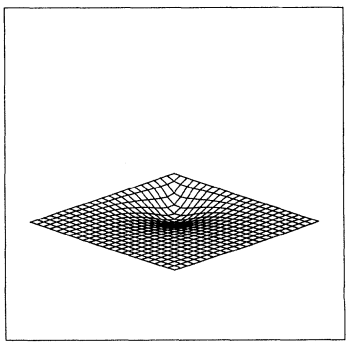

(1S1S) PAIR FUNCTION (L=1)

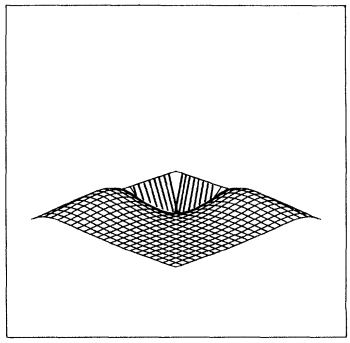

FIRST-ORDER FUNCTION FOR THE (1S1S) PAIR

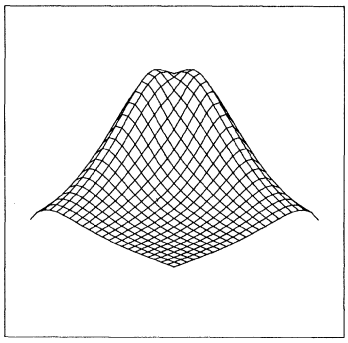

TOTAL FUNCTION FOR THE (1S1S) PAIR

FIG. 2. Perspective plots of the S and P waves and of zero-order, first-order, and total wave functions for the $(1s1s)$ pair.

The partial-wave contributions to the second-order energy have been calculated variationally by Byron and Joachain.[8] The contributions found by the two numerical approximations are compared to variational results in Tables VII-IX. For the $(1s1s)$ pair, the first three columns agree closely for each partial wave. The values of $E_2(1)$ and $E_2(2)$ predicted by Knight and Scherr[7] are less accurate, but their total second-order energy was not found by a partial-wave expansion and represents the most accurate value. The total E_2 given by

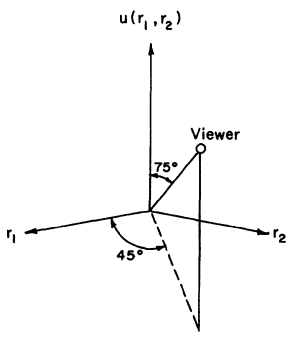

FIG. 3. Viewer's orientation for perspective plots.

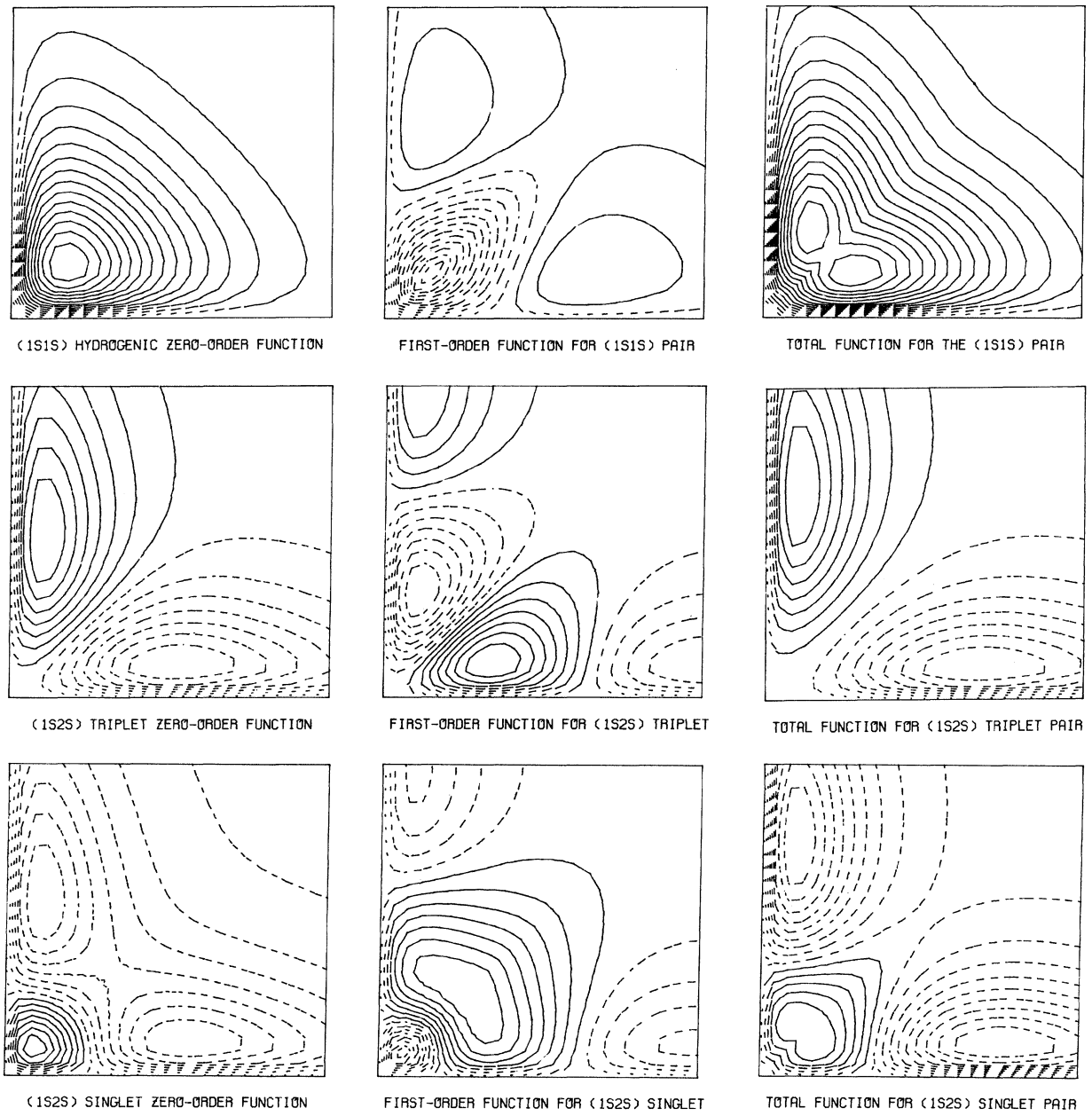

FIG. 4. Contour plots of zero-order, first-order, and total wave functions for the $(1s1s)\ ^1S$, $(1s2s)\ ^3S$, and $(1s2s)\ ^1S$ pairs.

Byron and Joachain contains contributions from partial waves not given in the table. The third-order energy shows somewhat worse agreement which is due in part to the finite number of partial waves used in the calculation. Comparison of the results for the ^3S and ^1S excited states illustrates the importance of the accurate difference formula and the increased cutoff. The agreement with Knight and Scherr[7] is generally better than for the ground state. In fact, Knight[9] recently reevaluated the ^1S second-order energy and found the improved value to be $-0.114\ 509\ 4$ a.u. This indicates that the fourth-difference value is the most accurate of those given in Table IX. The variational calculation of the partial-wave contributions by Byron and Joachain[8] compares less favorably for this pair. Since this is not the lowest state of its symmetry, it is expected that the variational method would have more difficulty. However, the main

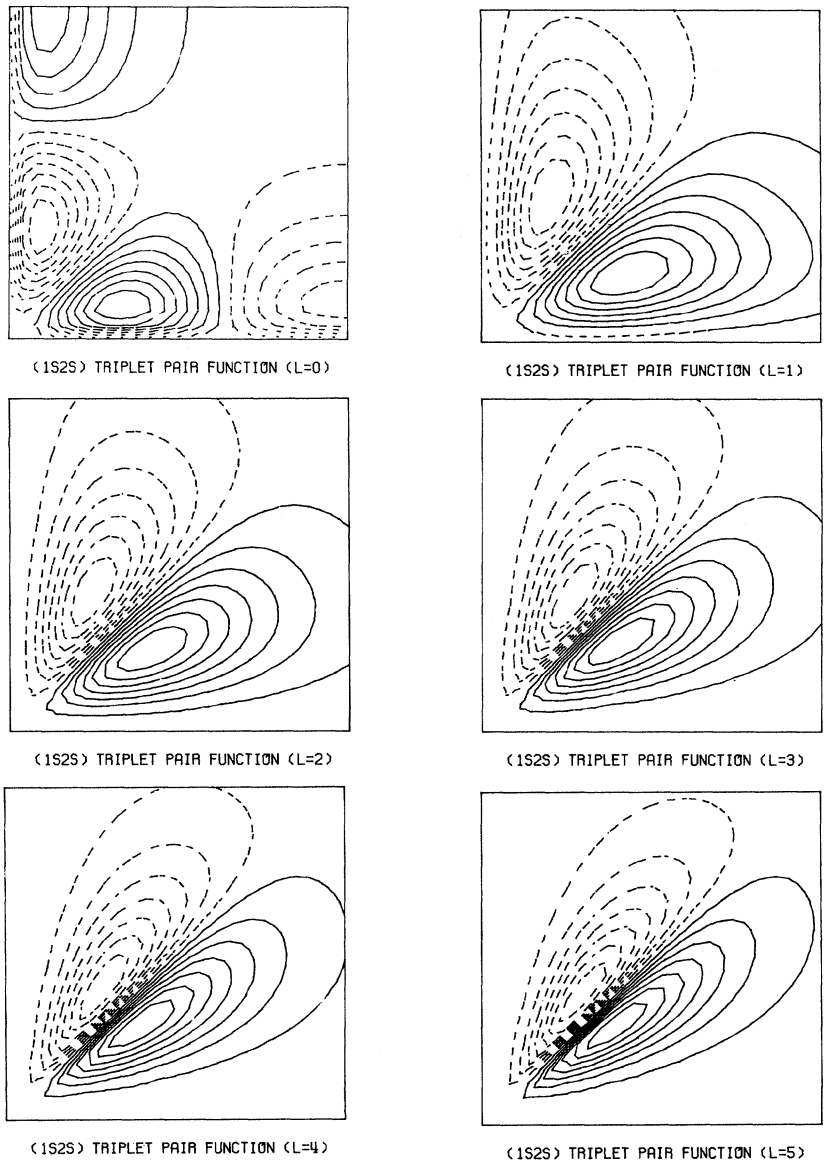

FIG. 5. Contour plots of functional coefficients for the $(1s2s)\ ^3S$ pair.

reason for the disagreement in this case is due to the choice of a configuration-interaction-type trial function for the functional coefficients.

Schwartz[10] gave an asymptotic formula for $E_2(l)$, which Byron and Joachain[8] used to estimate the contributions from partial waves with $l > 20$ for the ground state and with $l > 6$ for the excited states. They obtain $E_2(l > 10) = -0.000\,042$ a.u., $E_2(l > 6, {}^3S) = -0.000\,001$ a.u., and $E_2(l > 6, {}^1S) = -0.000\,041$ a.u. If the contribution for the ground state is added to the second-difference result, we obtain $-0.157\,661$ a.u., which agrees well with the correct value of $-0.157\,666$ a.u. The fourth-difference results predict that $E_2(l > 6, {}^3S) \simeq -0.000\,016$ a.u. and $E_2(l > 6, {}^1S) \simeq -0.000\,069$ a.u., using the accurate values of the second-order energy given by Knight[9] for comparison. Because the functional coefficients $u_l(r_1 r_2)$ are found as arrays of numbers, it is not possible to communicate them in a compact form. Each coefficient could be polynomial fitted, but these results would still require a large amount of space to display. However, qualitative information can be given in the form of contour plots of each pair function. The discussion of the plots of the functional coefficients for the three pairs is given in Sec. IV.

IV. CONTOUR AND PERSPECTIVE PLOTS OF PAIR FUNCTIONS

The numerical functions found on the linear grid were plotted over a square region with the boundaries set at one-half the radial cutoff. In each con-

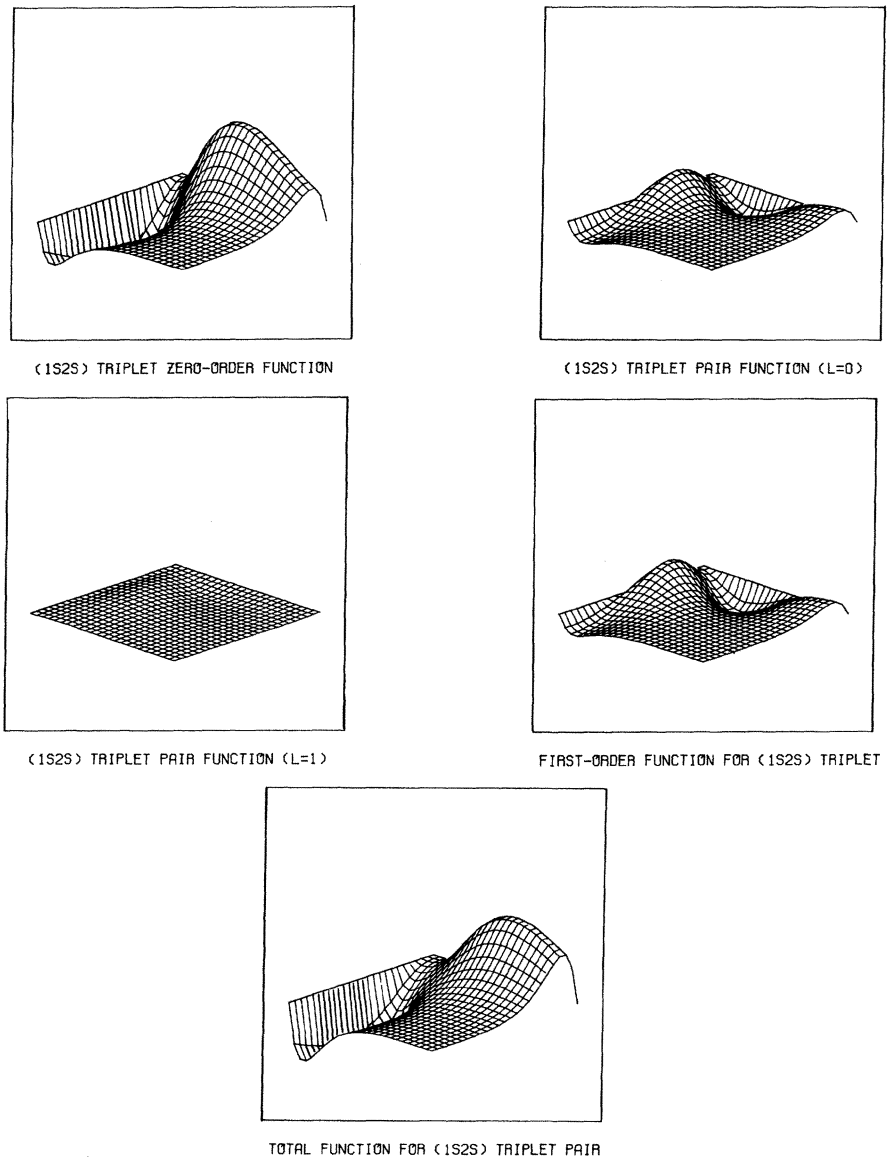

FIG. 6. Perspective plots of S and P waves and of the zero-order, first-order, and total wave functions for the $(1s2s)\,{}^3S$ pair.

tour plot, the nucleus is located at the lower left corner, with the r_1 and r_2 axes running horizontally and vertically from this point. The positive contours are given by solid lines and the negative contours by dashed lines. Because of an artifact of the Calcomp plotter, some of the solid lines tend to break up in regions of small r_1 or r_2. These should not be mistaken for negative contours, which are dashed lines in all regions. Each functional coefficient was multiplied by $r_1 r_2$ and plotted with a constant contour interval. The values of the contour interval and of the largest positive and negative contours for the three states are given in Table X. Ideally, these values should have been found for several grids and extrapolated to obtain quantitative results. Instead, the values are given for the particular function plotted and represent the exact results to no more than two or three significant figures.

Figure 1 gives the plots for the first six partial waves of the first-order function for the $(1s1s)$ pair. For $l=0$, the effect on the zero-order function is to subtract amplitude in the region close to the nucleus and along the line $r_1=r_2$. The functional coefficients for $l>0$ are negative in all regions, becoming more peaked along $r_1=r_2$, as l is increased. These waves have a simpler form, since the orthogonality to the zero-order function is ensured by the angular factor. In Fig. 2, the perspective plots of the first two partial waves are given along with the zero-order, first-order, and total functions. The viewer's orientation for these plots is shown in

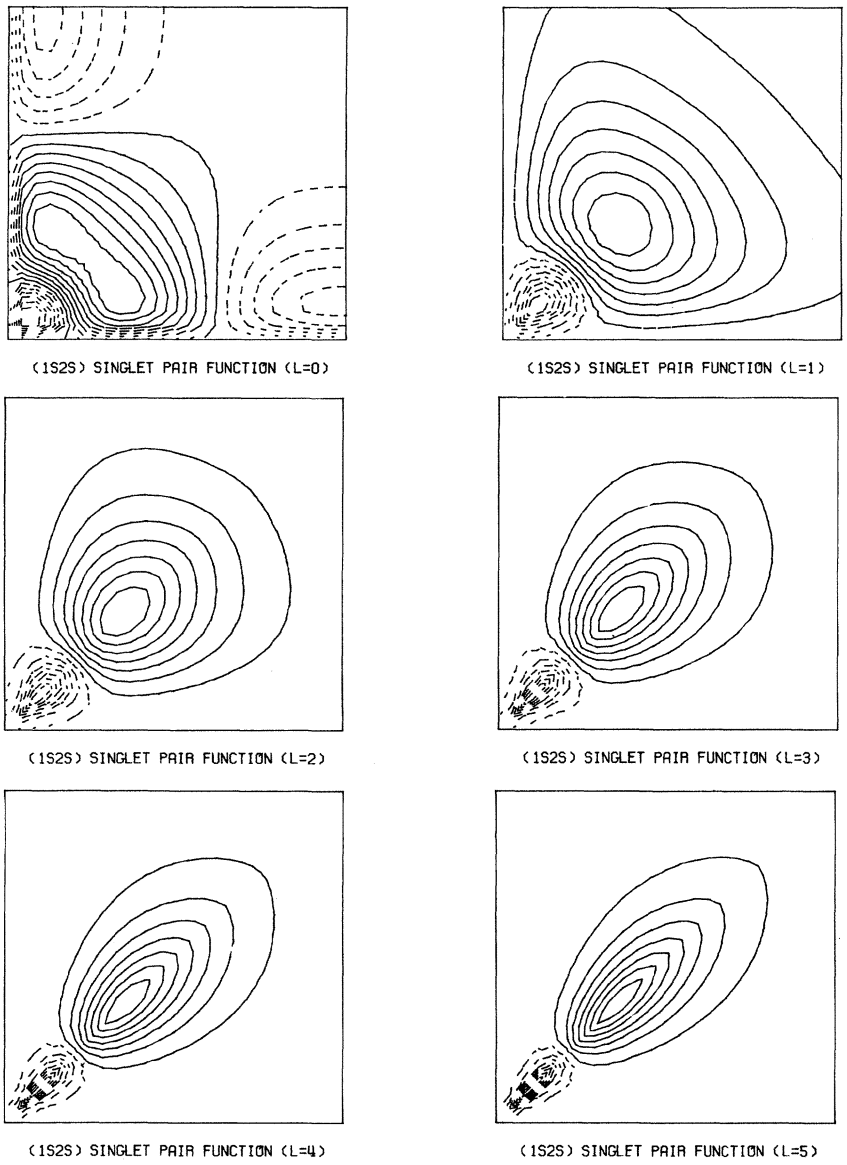

FIG. 7. Contour plots of functional coefficients for the $(1s2s)$ ^1S pair.

Fig. 3. Each perspective plot was drawn to the same scale and can be directly compared. The contour plots of ψ_0, ψ_1, and ψ for all three pairs are given in Fig. 4. The total first-order function was found by taking $\theta_{12}=0$ and summing the partial-wave components:

$$\psi_1=\sum_l u_l(r_1r_2); \tag{8}$$

then the total function was approximated by

$$\psi=\psi_0+\psi_1. \tag{9}$$

The first-order function shows a deep minimum near the nucleus and two well-separated maxima farther out. When this is added to the zero-order function, the total function is found to have two separated maxima with a minimum along $r_1=r_2$. This is qualitatively what the exact solution should look like.

The partial-wave contributions to the first-order function for the ^3S state are shown in Fig. 5. The trends are approximately the same as for the ground state except that the effects contributed by higher partial waves are smaller. This is expected because of the exact node at $r_1=r_2$. From the perspective plots of ψ_0 and ψ given in Fig. 6, the total first-order function serves to reduce the amplitude near the nucleus and increase it farther out (for the positive region). The contour plots of the functional coefficients for the ^1S excited state are shown in Fig. 7. They exhibit the intricate nodal structure expected for a state which is not the lowest of its symmetry. In each case, the functions subtract

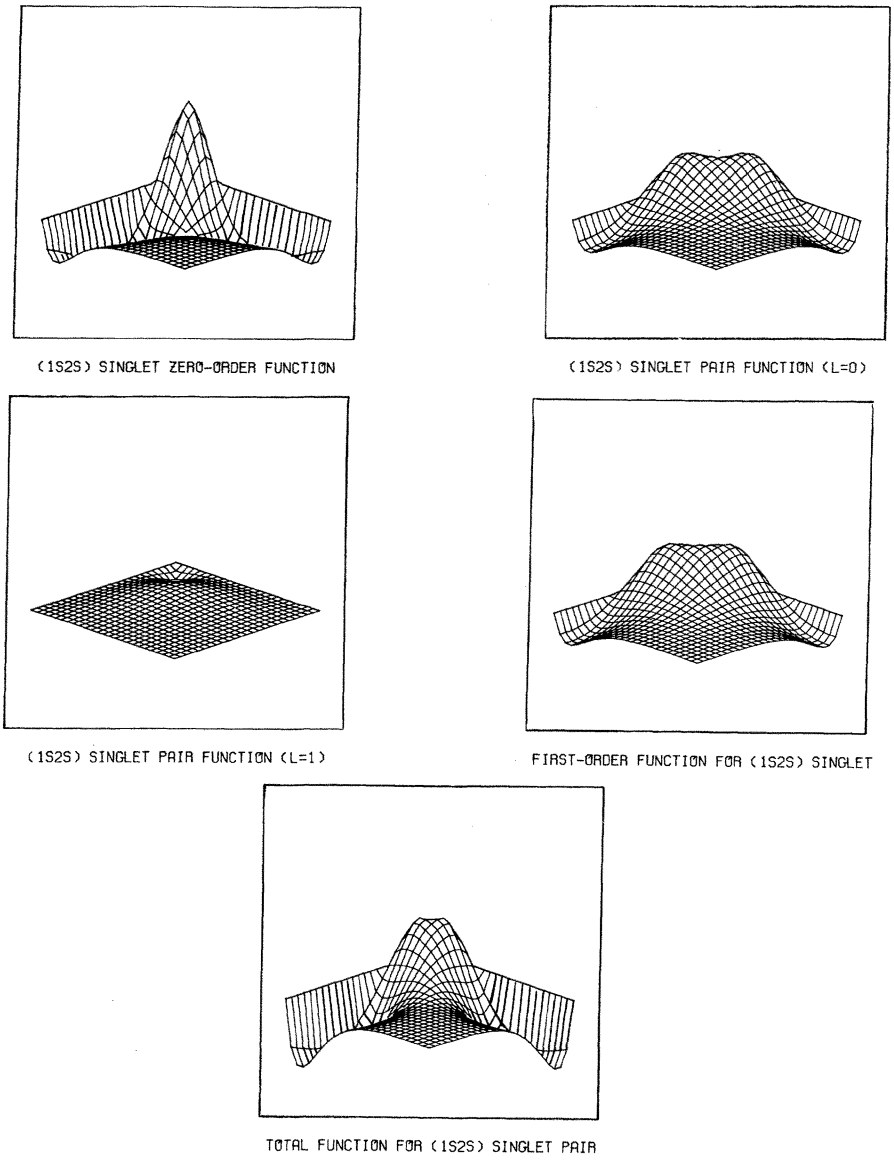

FIG. 8. Perspective plots of S and P waves and of zero-order, first-order, and total wave functions for the $(1s2s)\,{}^1S$ pair.

amplitude from the nuclear region and build amplitude in the region r_1, $r_2 \simeq 4$ a.u., when added to ψ_0. In Figs. 4 and 8, the zero-order function is shown to have a maximum at $r_1, r_2 \simeq 1$ a.u. and separated minima at $(r_1, r_2) \simeq (1, 6)$ a.u. and $(r_1, r_2) \simeq (6, 1)$ a.u. Adding the first-order function for $\theta_{12} = 0$, the total function has two maxima occurring at $(r_1, r_2) \simeq (1, 1.75)$ a.u. and $(r_1, r_2) \simeq (1.75, 1)$ a.u. The minima are moved out from 6 to 8 a.u. For both of the excited states, the perspective plots are drawn to the same scale as the ground state, so that amplitudes for the three states can be directly compared.

V. DISCUSSION

The MFD method has been shown to be capable of solving the first-order pair equations for the many-electron atom with accuracy comparable to the best variational results. In addition, because the method is not variational, it is quite easily applied to pairs that are not the first of their symmetry. The same programs that were used here for the $(1s1s)$ and $(1s2s)$ pairs can be applied without modification to any $(1sns)\,{}^{1,3}S$ pair. Since the results are independent of the nuclear charge, these pair functions can be used in the construction of the first-order wave function for any state of a general many-electron atom. In order to do this, the remaining pair functions, $(nsn's)$, $(npn'p)$, $(nsn'p)$, etc., where n may be the same as n', need to be calculated. These results will be reported in a

series of future papers. Once the total first-order wave function has been constructed from the set of pair functions, the total second- and third-order energy of the atom are easily calculated. The same quadrature and extrapolation techniques that are used for the pair energies can be applied, and the difficult integrals that have plagued the variation methods are avoided.

[1]V. McKoy and N. W. Winter, J. Chem. Phys. 48, 5514 (1968).

[2]O. Sinanoğlu, Advan. Chem. Phys. 6, 315 (1964).

[3]The first-order solutions for the $(1s2p)$ pairs have already been obtained and will be communicated in a future paper.

[4]N. W. Winter, D. Diestler, and V. McKoy, J. Chem. Phys. 48, 1879 (1968).

[5]N. W. Winter, A. Laferrière, and V. McKoy, Phys. Rev. A 2, 49 (1970).

[6]L. Richardson and J. Gaunt, Trans. Roy. Soc. (London) A226, 299 (1927); H. C. Bolton and H. I. Scoins, Proc. Cambridge Phil. Soc. 53, 150 (1956).

[7]R. E. Knight and C. W. Scherr, Rev. Mod. Phys. 35, 436 (1963).

[8]F. W. Byron and C. J. Joachain, Phys. Rev. 157, 1 (1967).

[9]R. E. Knight, Phys. Rev. 183, 45 (1969).

[10]C. Schwartz, Phys. Rev. 126, 1015 (1962).